Available online at www.sciencedirect.com
ScienceDirect
Thin Solid Films 515 (2007) 8764–8767
www.elsevier.com/locate/tsf

pH effect on the morphology of ZnO nanostructures grown with aqueous chemical growth

D. Vernardou [a,b,c,*], G. Kenanakis [a,d], S. Couris [e,f], E. Koudoumas [a,g], E. Kymakis [a,g], N. Katsarakis [a,b,h]

[a] Center of Materials Technology and Laser, School of Applied Technology, Technological Educational Institute of Crete, 710 04 Heraklion, Crete, Greece
[b] Science Department, School of Applied Technology, Technological Educational Institute of Crete, 710 04 Heraklion, Crete, Greece
[c] University of Crete, Department of Materials Science and Technology, 710 03 Heraklion, Crete, Greece
[d] University of Crete, Department of Chemistry, 710 03 Heraklion, Crete, Greece
[e] Institute of Chemical Engineering and High Temperature Chemical Processes (ICE–HT), Foundation for Research and Technology–Hellas (FORTH), 26504 Patras, Greece
[f] University of Patras, Department of Physics, 26504 Patras, Greece
[g] Electrical Engineering Department, Technological Educational Institute of Crete, 710 04 Heraklion, Crete, Greece
[h] Institute of Electronic Structure and Laser, Foundation for Research & Technology–Hellas, P.O. Box 1527, Vassilika Vouton, 711 10 Heraklion, Crete, Greece

Available online 1 April 2007

Abstract

ZnO nanostructures were grown for various pH values on Corning 7059 by aqueous chemical growth (ACG) using an equimolar aqueous solution of $Zn(NO_3)_2 \cdot 6H_2O$ (zinc nitrate hexahydrate) and $C_6H_{12}N_4$ (HMTA; hexamethylenetetramine). It was indicated that the increasing of the pH of the solution significantly leads to a modification of the ZnO morphology from rod-like to prism-like and flower-like structures.

Keywords: ACG; Nanostructures; ZnO; pH

1. Introduction

Zinc oxide (ZnO) is a well-known compound exhibiting a wide variety of interesting applications in photonic crystals [1], photodetectors [2], varistors [3] and solar cells [4]. Moreover, the synthesis and characterization of ZnO nanostructures have attracted great interest because of their significant applications in nanodevices [5,6].

ACG [7–9] is a quite simple technique for the deposition of nanostructures at relatively low temperatures, presenting several advantages such as the use of non-expensive equipment, the requirement of cheap and non-toxic reagents and the presence of non-hazardous by-products. Moreover, the morphological and structural characteristics of the grown samples can be controlled by adjusting parameters such as the concentration of the solution, the reagents stoichiometry, the temperature and the pH [10,11].

In this work, we investigate the possibility of controlling the nanostructures morphology grown using ACG by adjusting the pH of the solution. Towards this scope, preliminary results are presented related to the deposition of ZnO nanostructures on Corning 7059, at a deposition temperature of 95 °C, for a range of growth periods and various pH values.

2. Experimental

The growth of ZnO was performed on Corning 7059 employing ACG, using an equimolar (0.01 M) aqueous solution of $Zn(NO_3)_2 \cdot 6H_2O$ and HMTA as precursors. The solution and the substrate (positioned on top of a microscope glass stand) was placed in Pyrex glass bottles with polypropylene autocleavable screw caps and heated at a constant temperature of 95 °C for 1 h, 2 h and 5 h in a regular laboratory oven. The pH of the aqueous solution was adjusted using a 0.1 M NaOH solution. After each induction period, the samples were thoroughly washed with

* Corresponding author. Center of Materials Technology and Laser, School of Applied Technology, Technological Educational Institute of Crete, 710 04 Heraklion, Crete, Greece.
E-mail address: dvernardou@stef.teiher.gr (D. Vernardou).

0040-6090/$ - see front matter © 2007 Published by Elsevier B.V.
doi:10.1016/j.tsf.2007.03.108

MilliQ water in order to eliminate residual salts, and dried in air at a similar temperature (95 °C).

X-ray diffraction (XRD) measurements were performed using a Rigaku (RINT 2000) Diffractometer with Cu Kα X-rays, while Raman spectra were recorded using a T-64000 model of Jobin Yvon (ISA – Horiba group) with the 514.5 nm line of an air-cooled Ar^+ laser (Spectra-Physics 163-A42) operating at ~2 mW laser power for a total integration time of 300 s and the wavenumber range of 240–840 cm^{-1}. Finally, scanning electron microscopy (SEM) was performed on a Philips XL30 electron microscope. Each characterization method was completed on at least three samples prepared under the same conditions as well as on different areas of the same samples (front, centre, end and edges) for consistency and reproducibility.

3. Results and discussion

Fig. 1 presents the XRD patterns of ZnO deposited for 2 h at pH 7 and pH 8 on Corning 7059. The patterns exhibit all the characteristic peaks of the wurtzite ZnO hexagonal P6(3)mc structure, according to JCPDS card file No. 36-1451. No other peaks were observed, suggesting that only single-phase ZnO was formed. In addition, the phase of ZnO was found to be the same all along the surface of the sample, i.e. no variations in phase as a function of position on the substrate were observed. Similar patterns were recorded for other deposition times, provided that the pH value is kept the same. In contrast, no diffraction peaks were recorded for samples having pH values of 10 and 12, regardless the deposition time. In any case, as we will discuss in the Raman results, the ZnO wurtzite structure is also present in the samples grown at a pH of 10 and 12, however, the crystal quality is rather poor. The poor crystal quality for large pH values can be attributed to higher reaction rate, which was verified by the increasing of the precipitation rate of the solutions with increasing pH value.

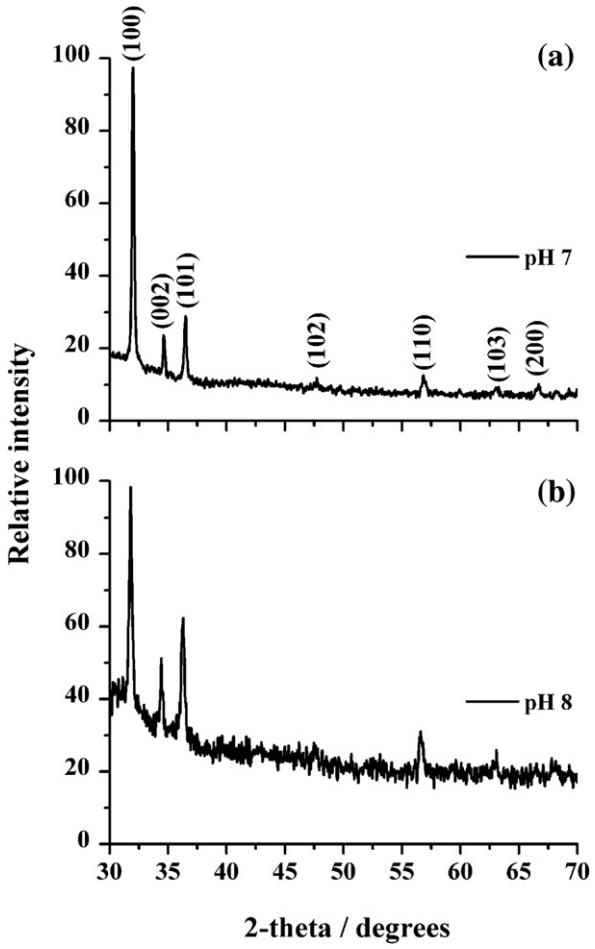

Fig. 1. XRD analysis of ZnO grown on Corning 7059 from a 10^{-2} M solution of $Zn(NO_3)_2 \cdot 6H_2O$ and HMTA at 95 °C for a deposition time of 2 h at (a) pH 7 and (b) pH 8.

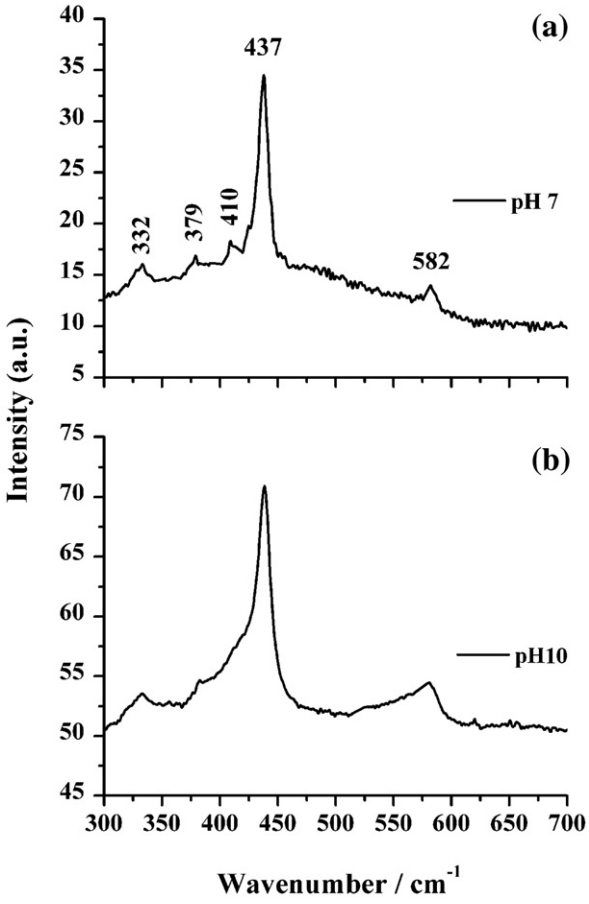

Fig. 2. Raman spectra of ZnO deposited on Corning 7059 using ACG at 95 °C for a deposition time of 2 h at (a) pH 7 and (b) pH 10.

The Raman spectra of the ZnO nanostructures grown at pH 7 and pH 10 are shown in Fig. 2(a) and (b), respectively (the corresponding Raman spectra for nanostructures grown at pH 8 and pH 12 are similar to those of pH 7 and pH 10, respectively). The observed phonon frequencies in these Raman spectra are: 332 cm^{-1} (multiple-phonon scattering processes), 379 cm^{-1} (A_1(TO)), 410 cm^{-1} (E_1(TO)), 437 cm^{-1} (E_2(high)) and 582 cm^{-1} (E_1(LO)), which are in excellent agreement with those reported in the literature [11]. The E_2(high) mode at 437 cm^{-1}, having the strongest intensity for all grown samples, is the characteristic of the ZnO hexagonal wurtzite structure [12]. Comparing Fig. 2(a) and (b) one can see that the increasing of pH induces a broadening of the E_2(high) mode, its full-width at

half-maximum (FWHM) being 7.32 cm^{-1} and 11.82 cm^{-1} for pH 7 and pH 10, respectively. The observed broadening is a strong indication that the crystal quality becomes poorer. Furthermore, the Raman peak at 582 cm^{-1} becomes stronger and much broader for samples grown at pH 10, indicating the presence of oxygen vacancies [13]. Therefore, the recorded Raman spectra clearly demonstrate that all ZnO nanostructured samples grown for various pH values have the hexagonal wurtzite structure, with no indications of impurities. Moreover, samples grown at pH 10 and pH 12 present poor crystal quality, a behaviour that was also confirmed by XRD.

SEM images of the ZnO nanostructures grown for 2 h on Corning 7059 from aqueous solutions at 95 °C and pH values of 7, 8, 10 and 12 are presented in Fig. 3. As can be seen, the morphology of the obtained ZnO nanostructures strongly depends on the pH of the solution. As an example, for pH 7,

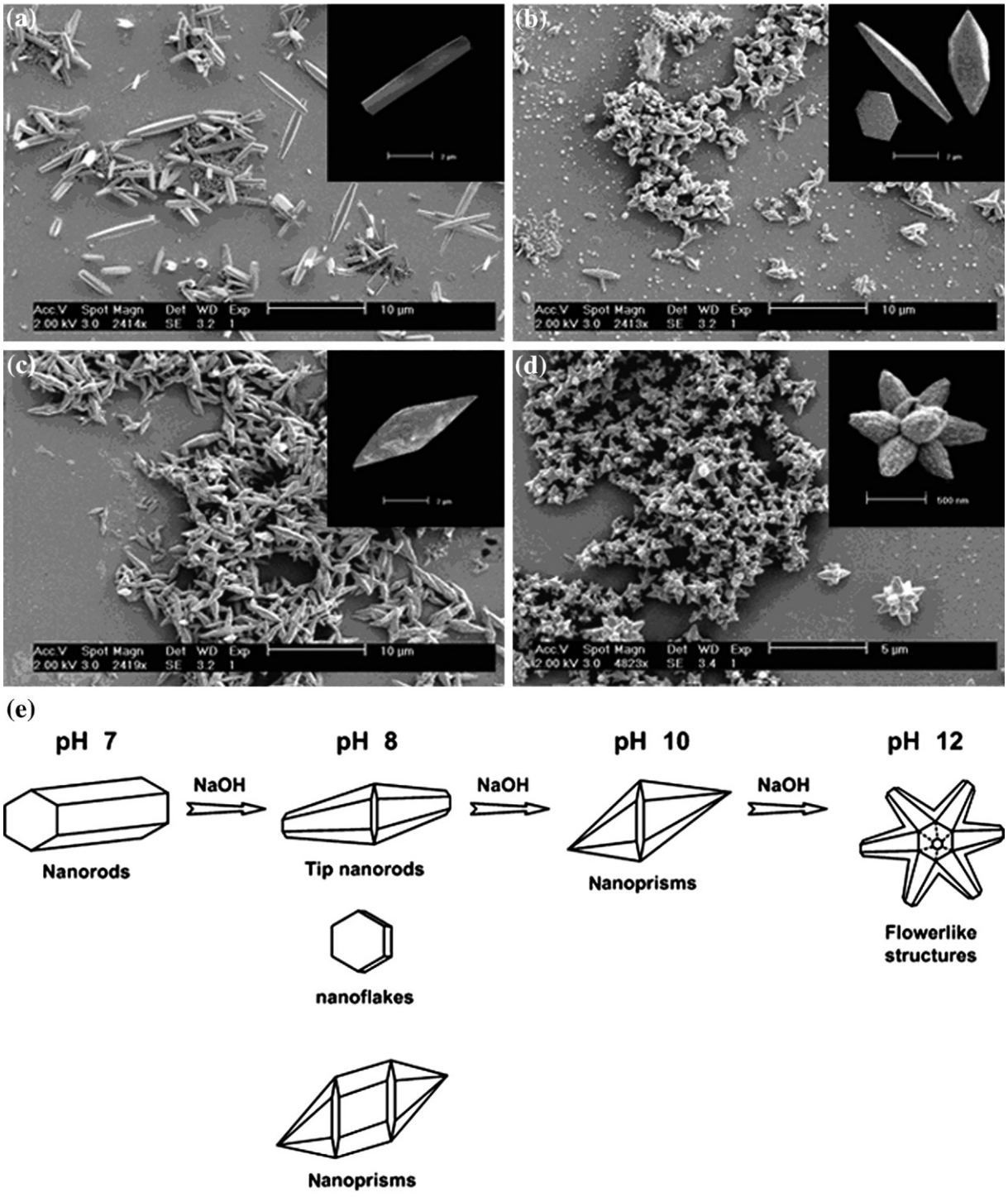

Fig. 3. SEM images of ZnO deposited on Corning 7059 using ACG for a deposition time of 2 h and (a) pH 7, (b) pH 8, (c) pH 10 and (d) pH 12. In the insets of (a), (b), (c) and (d), the individual structures are presented. Finally, (e) shows a schematic representation of the morphology of the nanostructures.

nanorods of approximately 5–6 μm length and 0.8–1 μm diameter can be obtained (Fig. 3a). Increasing the pH to a value of 8, a mixture of tip nanorods, nanoflakes and nanoprisms is grown (Fig. 3b), while only nanoprisms are present for pH 10 (Fig. 3c). Finally, as the amount of the NaOH solution further increases resulting in a pH of 12, flower-like structures consisting of nanoprisms are deposited (Fig. 3d). Following the above observations, it is clear that the morphological characteristics of as-prepared ZnO nanostructures are markedly controlled by the amount of NaOH. Moreover, as clearly observed in the insets of Fig. 3, although the shape of the nanostructures changes with increasing pH, their overall dimensions remain the same, at least for pH values up to 10. ZnO flowerlike structures grown at pH 12 exhibited smaller dimensions (length of about 500 nm), probably due to the higher precipitation rate, as mentioned earlier. Summarizing, the changes in the morphology of the ZnO nanostructures as a function of the pH value are schematically depicted in Fig. 3e. In any case, these are only preliminary results and further investigations, are required in order to clarify both the pH influence on the ZnO nanostructure morphology and the actual shape of the individual structures.

4. Conclusions

The pH effect on the morphological characteristics of ZnO nanostructures grown by ACG using $Zn(NO_3)_2 \cdot 6H_2O$ and HMTA as precursors at 95 °C for various deposition times was examined. It was found out that pH significantly influences the shape of the ZnO nanostructures, leading to a modification of the morphology from rod-like to prism-like and flower-like structures. Therefore, one can control the shape of the ZnO nanostructures by adjusting the pH of the solution. However, these are preliminary results and further investigation is required to verify the existing pH effect on the properties of ZnO samples and carry out kinetic studies of the system.

Acknowledgements

The authors would like to thank Ms Yang Yang and Professor Gehan Amaratunga from Department of Physics, University of Cambridge for providing the SEM images.

References

[1] Y. Chen, D. Bagnall, T. Yao, Mater. Sci. Eng., B, Solid-State Mater. Adv. Technol. 75 (2000) 190.
[2] S. Liang, H. Sheng, Y. Liu, Z. Hio, Y. Lu, H. Shen, J. Cryst. Growth 225 (2001) 110.
[3] M.H. Koch, P.Y. Timbrell, R.N. Lamb, Semicond. Sci. Technol. 10 (1995) 1523.
[4] C.R. Gorla, N.W. Emanetoglu, S. Liang, W.E. Mayo, Y. Lu, M. Wraback, H. Shen, J. Appl. Phys. 85 (1999) 2595.
[5] L.F. Dong, J. Jiao, D.W. Tuggle, J.M. Petty, S.A. Elliff, M. Coulter, Appl. Phys. Lett. 82 (2003) 1096.
[6] S.H. Jo, J.Y. Lao, Z.F. Ren, R.A. Farrer, T. Baldacchini, J.T. Fourkas, Appl. Phys. Lett. 83 (2003) 4821.
[7] L. Vayssieres, Adv. Mater. 15 (2003) 464.
[8] Q. Li, V. Kumar, Y. Li, H. Zhang, T.J. Marks, R.P.H. Chang, Chem. Mater. 17 (2005) 1001.
[9] X. Liu, Z. Jin, S. Bu, J. Zhao, K. Yu, Mater. Sci. Eng., B, Solid-State Mater. Adv. Technol. 129 (2006) 139.
[10] H. Zhang, D. Yang, S. Li, X. Ma, Y. Ji, J. Xu, D. Que, Mater. Lett. 59 (2005) 1696.
[11] Z. Zhaochun, H. Baibiao, Y. Yongqin, C. Deliang, Mater. Sci. Eng., B, Solid-State Mater. Adv. Technol. 86 (2001) 109.
[12] C. Roy, S. Byrne, E. McGlynn, J.-P. Mosnier, E. de Posada, D. O'Mahony, J.G. Lunney, M.O. Henry, B. Ryan, A.A. Cafolla, Thin Solid Films 436 (2003) 273.
[13] R. Al Asmar, J.P. Atanas, M. Ajaka, Y. Zaatar, G. Ferblantier, J.L. Sauvajol, J. Jabbour, S. Juillaget, A. Foucaran, J. Cryst. Growth 279 (2005) 394.